

FINITE-DIFFERENCE ALGORITHM FOR CONVECTION-DIFFUSION EQUATION APPLIED TO ELECTROPHORESIS PROBLEM

Sergey ERMAKOV, Olga MAZHOROVA,
Yuri POPOV

Keldysh Institute of Applied Mathematics
USSR Academy of Sciences
125047 Moscow, Miusskaya sq.4, USSR

Abstract. Finite-difference algorithm for solving convection-diffusion equation with small coefficient at Laplace operator is developed. It is based on equivalent partial differential equation approach. Both linear and nonlinear equations are considered and appropriate finite-difference schemes are proposed. Some analysis of their properties is conducted. The computational efficiency of this algorithm is studied using various test problems. Some results on numerical simulation of capillary isotachophoresis is presented.

Key words: finite-difference scheme, differential approximation, dispersion, electrophoresis, sample, mobility.

1. Introduction. The phenomenon of electrophoresis (when charged particles are transported under the impact of electric field) has long been used in practice. Many substances, when dissolved in water, dissociate, i.e., decompose into ions or accept/donate protons. Neutral molecules as well as large formations (colloidal particles, cells) become charged and get into directed motion under the impact of electric field. The velocity of the steady motion \vec{V} is proportional to the intensity of electric field \vec{E} , the proportionality factor is called the mobility γ , i.e.,

$$\vec{V} = \gamma \cdot \vec{E} . \quad (1)$$

The latter depends on the particle charge and geometry, the viscosity of the outer medium and some other factors. It is an individual

characteristic of a substance. Different mobilities for different substances is in fact underlying the electrophoretic separation of many biological objects.

There are several techniques for electrophoretic separation of biomixtures (Deyl, 1979). Let us mention two of them. Suppose that sample has low concentration compared to that of buffer solution which it is placed in. Moving with different velocities under the electric field impact, the sample species will spatially separate from each other. The starting position of the sample, called the zone, will divide into several zones, containing individual substances. This is the main idea of so called zone electrophoresis (ZE) technique. In the other technique electrolytes are organized in separation column in a special manner. Sample species are placed between the leader, an electrolyte which has the ion with the highest mobility, and terminator, which has the ion with the lowest one. After applying the electric field, this system gets into motion. The sample species separate forming up the train behind the leader in decreasing order of mobility. When the separation process is finished all species are moving with the same velocity, set by the leader. That is why the technique is called isotachopheresis (ITP).

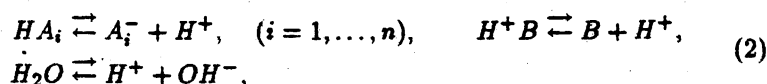
Currently there are several mathematical models of electrophoresis (Babskii et al., 1989; Bier et al., 1983; Saville et al., 1986; Mosher et al., 1989; Roberts et al., 1989). All of them are based on the mass conservation law, written for each sample component and buffer solution; the charge conservation law, the assumptions on electric neutrality and local chemical equilibrium. Systems of equations, obtained in these models are rather similar, however they have been solved only for the simplest 1-D cases. In particular Zhukov (1984) obtained an analytical solution describing the dynamics of mixture separation by isotachopheresis. He considered both weak and strong electrolytes and neglected diffusion transport. The effect of different initial conditions upon the resulting separation in the system of four electrolytes was numerically analyzed in the approximation of strong electrolytes (Fidler et al., 1985). A behavior of the boundary between electrolytes and its stability in the ITP

method were studied by (Moshier et al. 1985), while the mechanisms affecting on the separation quality in ZE were considered by (Roberts et al., 1989).

The above mathematical models may be implemented in installations with separation chambers of different geometries. However last time the capillary electrophoresis, when separation occurs in a thin capillary, has been of particular interest. Further we shall consider exactly this kind of electrophoresis.

In this paper a number of numerical algorithms are considered to satisfy some specific requirements, arising in capillary ITP simulation. To solve the transport equation with a small coefficient at the second derivative a finite-difference scheme with artificial dispersion was developed. Unlike Fidler et al. (1985) we do not assume that all electrolytes are fully dissociated.

2. Mathematical model of electrophoresis. We consider a thin capillary filled up with aqueous solution of n monovalent acids and one monovalent base. The last one is a counterion. We assume that capillary is thermally stabilized and that the liquid is in mechanical equilibrium. Then the problem is reduced to 1-D case where concentrations of individual components will be determined by chemical reactions in the system, electrophoretic migration and diffusion. The dissociation-association reactions of the acids, base and water have schemes:



where HA_i, B - neutral acid and base molecules, $A_i^-, H^+ B, H^+, OH^-$ - acid, base, hydrogen and hydroxyl ions respectively. Since the rate of chemical reactions is much higher compared to the transport processes (electrophoretic migration, diffusion), we can use the local chemical equilibrium hypothesis. It implies that chemical equilibrium exists at every point in space and time. Hence it is convenient to use analytical concentrations $a_i, [H^+]$, specified as

$$a_i = [HA_i] + [A_i], \quad \alpha_i = \frac{[A_i^-]}{a_i} = \frac{K_i}{K_i + [H^+]}, \quad (i = 1, \dots, n); \quad (3)$$

$$a_0 = [H^+B] + [B], \quad \alpha_0 = \frac{[H^+B]}{a_0} = \frac{[H^+]}{K_0 + [H^+]},$$

where [] - molar concentration, $K_i, \alpha_i (i = 0, \dots, n)$, - equilibrium constant for i -th reaction and dissociation degree for the i -th electrolyte respectively. In this case there is no more need to consider the chemical reactions. Finally, adopting the electric neutrality hypothesis we may write a system of dimensionless equations for ITP (Zhukov, 1984):

$$\frac{\partial a_i}{\partial t} + \frac{\partial}{\partial x} \{ z_i \cdot \alpha_i \cdot \gamma_i \cdot a_i \cdot E \} = \frac{1}{Sc_i} \cdot \frac{\partial^2 a_i}{\partial x^2}, \quad i = 0, \dots, n, \quad (4)$$

$$j = \sum_{i=0}^n \left\{ -\frac{1}{Sc_i} \cdot \frac{\partial(z_i \cdot \alpha_i \cdot a_i)}{\partial x} + z_i^2 \cdot \alpha_i \cdot \gamma_i \cdot a_i \cdot E \right\} - \frac{1}{Sc_{n+1}} \cdot \frac{\partial[H^+]}{\partial x} + \frac{1}{Sc_{n+2}} \cdot \frac{\partial[OH^-]}{\partial x} + \{ \gamma_{n+1} \cdot [H^+] + \gamma_{n+2} \cdot [OH^-] \} \cdot E, \quad (5)$$

$$\sum_{i=0}^n z_i \cdot \alpha_i \cdot a_i - [OH^-] + [H^+] = 0, \quad (6)$$

$$Sc_i = \frac{j^* \cdot L \cdot e}{k_B \cdot T \cdot a^* \cdot F \cdot \gamma_i}, \quad i = 0, 1, \dots, n+2. \quad (7)$$

Here $z_i, D_i, \gamma_i (i = 0, \dots, n+2)$, - charge, diffusion coefficient and ion mobility per unit charge; E - the intensity of electric field; F and k_B - are Faraday and Boltzmann constant respectively; j - the electric current density; T - temperature; t - time; e - the charge of electron. Spatial coordinate x is measured along capillary. To obtain the dimensionless equations the following formulas are used: $\tilde{a}_i = a^* \cdot a_i (i = 0, 1, \dots, n)$, $\tilde{x} = L \cdot x$, $\tilde{\gamma}_i = \gamma^* \cdot \gamma_i (i = 0, 1, \dots, n+2)$, $\tilde{j} = j^* \cdot j$, $\tilde{t} = (F \cdot L \cdot a^* / j^*) \cdot t$, $\tilde{E} = j^* \cdot (F \cdot a^* \cdot \gamma^*)^{-1} \cdot E$, where a^*, L, j^*, γ^* - are the concentration, length, current density and mobility scales (dimension variables are marked with a wave). Subscripts $i = 1, 2, \dots, n$ correspond to acids, $i = 0$ - to base, $i = (n+1)$ and $i = (n+2)$ denote hydrogen and hydroxyl ions. We also assume the Einstein relation for the diffusion coefficients to be valid:

$$D_i = \frac{k_B \cdot T \cdot \gamma_i}{e}. \quad (8)$$

Equations (4) describe the transport of individual components, the relation (5) represents the continuity equation for electric current, and the relation (6) is based on the assumption of the electric neutrality of the medium. The latter is used for calculating the concentration of hydrogen ion $[H^+]$. In this case we assume that the current density $j = j(t)$ is given, and the hydroxyl ion concentration may be determined using the water ionic product:

$$[OH^-] = \frac{K_w^2}{[H^+]}, \quad (9)$$

where $K_w^2 = 10^{-14} \text{ mol}^2 \cdot L^{-2}$.

The system (4)–(6) includes $(n + 3)$ equations where (4) are quasilinear partial differential equations, while (5) and (6) are linear and nonlinear algebraic equations respectively. Taking into account (3) and (9) the set (4)–(6) contains $(n + 3)$ unknown variables: $a_i (i = 0, \dots, n)$, E , $[H^+]$. We assume that the initial concentration profiles along capillary are known for all components, and the current density is fixed. We also suppose that capillary is long enough and the concentrations of leader and terminator are supported constant at its corresponding ends. Now one can believe that the problem is quite definite.

The dimensionless Schmidt number Sc_i describes the relation between the electrophoretic transport and diffusion. For real conditions $Sc_i \simeq 10^3 \div 10^4$, while the coefficient at Laplace operator in (4) has the order of $10^{-3} \div 10^{-4}$. Hence, the contribution of diffusion is rather small and it may be ignored in the first approximation, as Zhukov (1984) did. The aim of this study is to estimate the diffusion effect on the dynamics of separation process and the width of transition region between two electrolytes.

3. Numerical algorithm. It is well known that solving the convection-diffusion equations with a small parameter at the second derivative, such as equation (4), we meet some difficulties. Using conventional finite-difference schemes (FDS) one may obtain the solution of satisfied accuracy only on the difference grids with spatial steps $h \sim 1/N \sim 1/Sc$ (where N is the number of grid points

in one spatial dimension). For large Sc it results in considerable computational expenses. In this section we describe FDS with artificial dispersion. It was developed using differential approximation method (Shokin et al., 1985), which is also known as equivalent partial differential equation analysis. This FDS allows to fulfill computations with larger steps and hence to reduce computational time. Earlier this method was applied to develop the FDS with artificial dispersion for Euler equations (Muhin et al., 1981) and for the linear convection-diffusion equation (Mazhorova et al., 1986).

3.1. Linear problem. Let us outline the FDS with artificial dispersion for convection-diffusion equation with constant transport velocity u . We consider Cauchy problem for 1-D equation

$$\frac{\partial C}{\partial t} + u \cdot \frac{\partial C}{\partial x} = D \cdot \frac{\partial^2 C}{\partial x^2}, \quad (10)$$

where $u = 1$, $D \ll 1$ - the dimensionless coefficient; $-\infty < x < +\infty$, $t > 0$, $C(x, 0) = C_0(x)$. The uniform space and time finite difference grid with constant steps h and τ is introduced. We also apply some standard notations:

$$\begin{aligned} C_i &= C(x_i, t_h), \quad \hat{C}_i = C(x_i, t_{n+1}), \quad C_i^{(\sigma)} = \sigma \cdot \hat{C}_i + (1 - \sigma) \cdot C_i, \\ C_t &= \frac{\hat{C}_i - C_i}{\tau}, \quad C_x = \frac{C_{i+1} - C_i}{h}, \quad C_x = \frac{C_i - C_{i-1}}{h}, \\ C_x &= \frac{C_{i+1} - C_{i-1}}{2h}, \quad C_{xx} = \frac{C_{i+1} - 2 \cdot C_i + C_{i-1}}{h^2}. \end{aligned} \quad (11)$$

Using these abbreviations we write down the simplest FDS for equation (10), where the convective term is approximated by upwind C_x (12) and central C_x (13) differences:

$$C_i + u \cdot C_x^{(\sigma)} = D \cdot C_{xx}^{(\sigma)}, \quad (12)$$

$$C_i + u \cdot C_x^{(0.5)} = D \cdot C_{xx}^{(0.5)}. \quad (13)$$

FDS with upwind difference has considerable dissipative properties resulting from the presence of additional scheme diffusion of

spurious nature. Its value may be estimated by deriving the differential approximation (DA) for (12) with the second order accuracy, omitting the terms of the order of $O(h^2 + \tau^2)$:

$$\frac{\partial C}{\partial t} + u \cdot \frac{\partial C}{\partial x} - (D + D_{sch}) \cdot \frac{\partial^2 C}{\partial x^2} = 0. \quad (14)$$

Here $D_{sch} = \frac{1}{2} \cdot u \cdot h + (\sigma - \frac{1}{2}) \cdot u^2 \cdot \tau$. A part of scheme diffusion may be eliminated by setting $\sigma = \frac{1}{2}$. (Further we shall consider only FDS with $\sigma = \frac{1}{2}$). Then $D_{sch} = \frac{1}{2} \cdot u \cdot h$, and in fact (12) approximates the equation (10) but with diffusion coefficient $\tilde{D} = D + D_{sch}$. This may lead to considerable loss of accuracy for small D and large h . An influence of scheme diffusion D_{sch} will be insignificant if $h < 2 \cdot D/u$, but for small D it will require very fine grids, that results in the increase of computations.

Deriving the DA for the FDS (13) with $O(h^3 + \tau^3)$ order of accuracy and assuming $\sigma = \frac{1}{2}$ we may convince that the scheme diffusion is absent. However the dispersion term with the third order derivative of the solution appears

$$\frac{\partial C}{\partial t} + u \cdot \frac{\partial C}{\partial x} - D \cdot \frac{\partial^2 C}{\partial x^2} + u \cdot Q \cdot \frac{\partial^3 C}{\partial x^3} = 0, \quad (15)$$

where $Q = \frac{1}{6} \cdot (h^2 + \frac{1}{2} \cdot \tau^2 \cdot u^2)$. Equation (15) is the linearized Korteweg-de Vries-Burgers equation. Spurious oscillations arising in solution within the regions of sharp gradients, when the FDS (13) is used, are caused by the presence of scheme dispersion $u \cdot Q \cdot \partial^3 C / \partial x^3$ (see for example Mazhorova et al. (1986)). To reduce its negative influence on solution we introduce an antidispersion term into FDS (term approximating $u \cdot Q \cdot \partial^3 C / \partial x^3$ with opposite sign). Therefore consider the following FDS:

$$C_i + u \cdot C_p^{(0.5)} - D \cdot C_{xx}^{(0.5)} - u \cdot Q \cdot [\kappa \cdot C_{xxx}^{(\sigma)} + (1 - \kappa) \cdot C_{xxx}^{(\sigma)}] = 0. \quad (16)$$

Here

$$C_{xxx} = \frac{C_{i+2} - 3 \cdot C_{i+1} + 3 \cdot C_i - C_{i-1}}{h^3},$$

$$C_{xxx} = \frac{C_{i+1} - 3 \cdot C_i + 3 \cdot C_{i-1} - C_{i-2}}{h^3}.$$

The parameter κ determines the form of the third derivative approximation. When $\kappa = 0$ it is upwind third difference, when $\kappa = 0.5$ it is central third difference. Writing the scheme (16) we use the extended 10-point computational stencil, but it is also possible to write the FDS with artificial dispersion on conventional 6-point stencil. For this purpose, we may transform the dispersion term $u \cdot Q \cdot \partial^3 C / \partial x^3$ using the eq. (10) and omitting the higher order terms:

$$-Q \cdot \frac{\partial^3 C}{\partial x^2 \partial t}$$

Then the FDS with artificial dispersion looks like

$$C_t + u \cdot C_x^{(0.5)} - D \cdot C_{xx}^{(0.5)} + Q \cdot C_{xxt} = 0. \quad (17)$$

Let us compare the properties of FDSs (12), (13), (16) and (17) for the test problem with the following initial conditions:

$$C_0(x) = \begin{cases} 1 & \text{at } x \leq 0 \\ 0 & \text{at } x > 0 \end{cases} \quad (18)$$

for which the analytic solution of (10) is given by the formula

$$\bar{C}(x, t) = \frac{1}{\sqrt{\pi}} \left\{ \frac{\sqrt{\pi}}{2} - \int_0^{\frac{(x-u)t}{2\sqrt{Dt}}} e^{-z^2} dz \right\} = \frac{1}{2} - \frac{1}{2} \cdot \operatorname{erf} \left[\frac{x - u \cdot t}{2\sqrt{D \cdot t}} \right]. \quad (19)$$

We shall use it to estimate the accuracy of numerical solutions.

The computational results obtained by FDSs (12), (13), (17) and (16) with $\kappa = 0$ and $\kappa = 0.5$ respectively are shown in Fig. 1-5. The solid lines represent the calculated profiles of concentration while the dashed lines correspond to analytical solution (19). The profiles are plotted for $t = 0.05$, $t = 0.4$, $t = 2.0$ with $u = 1$, $h = 10^{-2}$, $\tau = 5 \cdot 10^{-3}$, $D = 2 \cdot 10^{-4}$ and $\sigma = 0.5$.

The FDSs with artificial dispersion (16)-(17) give the opportunity, on one hand, to avoid strong spreading of concentration shock (like in FDS (12) with upwind differences) and, on the other hand, to reduce spurious oscillations of solution within the region of sharp gradients (typical for (13)). Oscillations initially arising

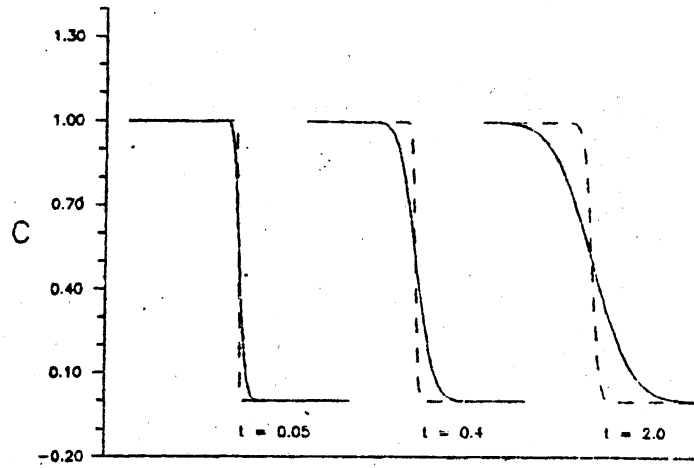


Fig. 1. Concentration profiles : analytical solution - - - - ;
computed solution obtained using FDS (12) _____ .

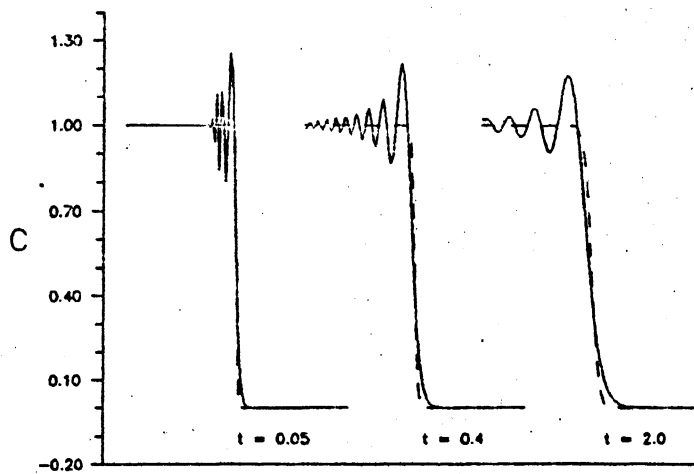


Fig. 2. Concentration profiles : analytical solution - - - - ;
computed solution obtained using FDS (13) _____ .

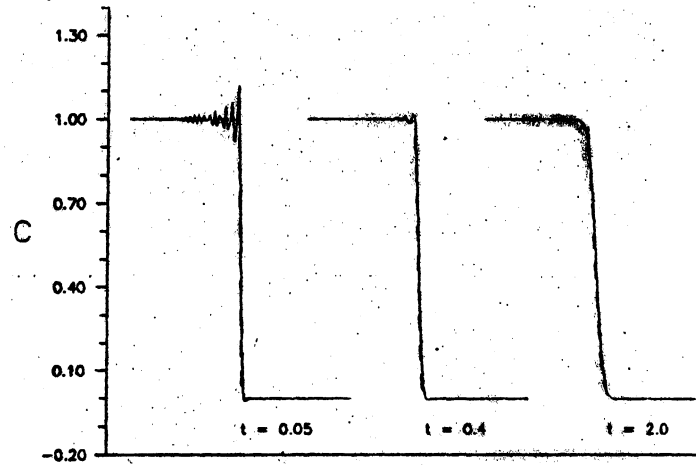


Fig. 3. Concentration profiles : analytical solution ----- ;
computed solution obtained using FDS (17) _____.

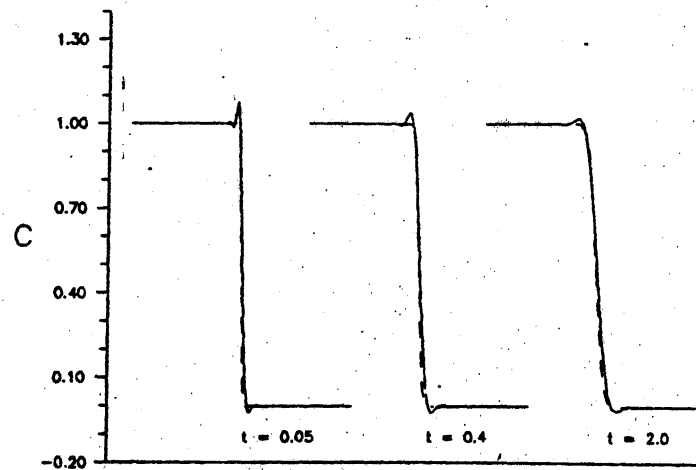


Fig. 4. Concentration profiles : analytical solution ----- ;
computed solution obtained using FDS (16) with
 $\alpha = 0.0$ _____.

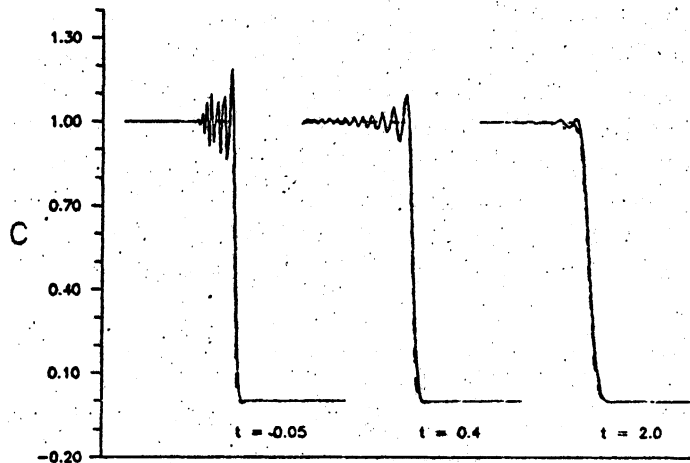


Fig. 5. Concentration profiles : analytical solution - - - - - ;
 computed solution obtained using FDS (16) with
 $\kappa = 0.5$ ——— .

in solution obtained by FDSs (16)–(17) damp rather quickly. The number and the amplitude of these oscillations in solution (16) depend on value of the parameter κ : with the decrease of κ from 0.5 to 0 their number is reduced and at $\kappa = 0$ only two of them retain. One "negative" peak (i.e., with negative C value) locates in front of concentration jump and another "positive" one is behind it (Fig. 4).

This difference between the solutions obtained by FDSs (17) and (16) with $\kappa = 0$ and $\kappa = 0.5$ may be explained by considering DA of these schemes with truncation error $O(h^3 + \tau^3)$

$$\frac{\partial C}{\partial t} + u \cdot \frac{\partial C}{\partial x} - D \cdot \frac{\partial^2 C}{\partial x^2} + R \cdot \frac{\partial^4 C}{\partial x^4} = 0, \quad (20)$$

where $R = R_{(17)} = \frac{1}{6} \cdot \left[\frac{D \cdot h^2}{2} - D \cdot \tau^2 \cdot u^2 \right]$ for scheme (17)

and $R = R_{(16)} = u \cdot Q \cdot \left[\frac{(1-2\kappa) \cdot h}{2} + \tau \cdot u \cdot \sigma \right] - \frac{1}{4} \times \left[\tau^2 \cdot u^2 \cdot D + \frac{h^2 \cdot u^2 \cdot \tau}{2} + \frac{h^2 \cdot D}{2} + \frac{u^2 \cdot \tau^3}{6} \right]$ for scheme (16).

Forth derivative term $R \cdot \partial^4 C / \partial x^4$ is available in DA of both schemes. Coefficient R depends on spatial and time grid steps (h and τ) at

fixed u and D . It also depends on weight parameters κ and σ in FDS (16). When $R > 0$ this term produces the dissipative, smoothing effect on solution, while for $R < 0$ its effect is opposite. The absolute value of coefficient R determines the magnitude of effect.

All these statements are proved by results displayed in Fig. 1-5. It's easy to convince that $R_{(16)}$ and $R_{(17)}$ corresponding to FDS (16) with $\kappa = 0$ (Fig. 4) and FDS (17) (Fig. 3) are positive. Taking into account that $\tau = h/2$ they are equal to

$$R_{(17)} = \frac{D \cdot h^2}{24}, \quad R_{(16)} = \frac{3 \cdot h^3}{32} - \frac{7 \cdot D \cdot h^2}{48} \simeq \frac{3 \cdot h^3}{32} \quad \text{since } D \simeq h^2.$$

In both FDSs the term with the fourth derivative produces the smoothing effect which is more considerable for (16) since

$$R_{(16)}/R_{(17)} \simeq 9 \cdot h/(4 \cdot D) \gg 1.$$

However the increase of dissipative term together with suppressing of oscillations leads to the loss of accuracy, which is particularly noticeable by $t = 2.0$. By this time the solution obtained by (17) is closer to the exact one than the solution obtained by (16).

When $\kappa = 0.5$ the fourth derivative term produces negative effect on solution (Fig. 5), because in this case $R_{(16)} = -7 \cdot D \cdot h^2/48$. The amplitude of oscillations increases and they spread over larger area (compare with Fig. 3 since $|R_{(17)}| \simeq |R_{(16)}(\kappa = 0.5)|$). Thus comparing three FDSs with artificial dispersion we may suggest that FDS (16) with $\kappa = 0$ suppresses the oscillations better than the other two.

It's easy to show that adding the antidispersion term to FDS (16) with $\kappa = 0$ we change the coefficients in the system of linear equations so that it improves the diagonal domination in matrix of coefficients. Hence this term improves the computational stability, what is very important. On the contrary additional term in (17) reduces the stability. Some methodical calculations for different D and h values show that the scheme (16) with $\kappa = 0$ is sufficiently accurate and it doesn't yield oscillations if $D/h^2 \geq 1$, unlike the FDS (17), which gives oscillating solutions.

We have attempted to estimate the computational efficiency of FDS (16) comparing it with oscillation free FDS (12), on the basis of test problem described earlier. We assumed that computational efficiency was determined first of all by computer time expenses required for achieving the prescribed accuracy. For criterion the following parameter $\varepsilon^{(N)} = \max_i |\bar{C}_i - C_i^{(N)}|$ (\bar{C} —the analytical solution (19) and $C_i^{(N)}$ —the numerical solution, obtained using FDS (N)) was taken. Here subscript i below max function means that maximum value was searched for all grid points. The solution $C_i^{(16)}$, displayed in Fig. 4, and $\varepsilon^{(16)}$ were chosen as a reference. Solving (10) with FDS (12) at different h and τ steps we had to obtain the identical error value $\varepsilon^{(16)}$ for FDS (12) solution. Making a series of computations with finer and finer grids we've found that $\varepsilon^{(16)}$ and $\varepsilon^{(12)}$ were approximately equal for both solutions at $h = 2.5 \cdot 10^{-4}$, i.e., 40 times smaller than for (16). Simultaneously for computations to be stable we had to decrease the time step τ . As result we've obtained total saving of time as much as 420 to 1. This advantage increases with the decrease of coefficient D .

3.2. Nonlinear problem. Now consider the case when transport velocity depends on the substance concentration $u = u(C)$. For the equation

$$\frac{\partial C}{\partial t} + \frac{\partial(u \cdot C)}{\partial x} = D \cdot \frac{\partial^2 C}{\partial x^2} \quad (21)$$

we write down the FDS

$$C_i + (W_{i+1/2}^{(0.5)} - W_{i-1/2}^{(0.5)})/h = D \cdot C_{xx}^{(0.5)}, \quad (22)$$

where $W^{(0.5)} = u \cdot C^{(0.5)}$ —is convective flux, $W_{i+1/2}^{(0.5)} = 1/2 \cdot (W_{i+1}^{(0.5)} + W_i^{(0.5)})$. As before we shall assume that the dimensionless coefficient $D \ll 1$. In FDS (22) the velocity u will refer to the previous time layer so that a resulting system of equations would be linear. The DA of (22) derived on uniform space and time grid with the order of accuracy $O(h^3 + \tau^3)$ has form:

$$\begin{aligned}
& \frac{\partial C}{\partial t} + \frac{\partial(u \cdot C)}{\partial x} - D \cdot \frac{\partial^2 C}{\partial x^2} + \frac{h^2}{6} \cdot \frac{\partial^3(u \cdot C)}{\partial x^3} - \frac{h^2}{4} \cdot \frac{\partial}{\partial x} \left[\frac{\partial u}{\partial x} \cdot \frac{\partial C}{\partial x} \right] \\
& - \frac{\tau^2}{12} \cdot \frac{\partial}{\partial x} \left[u \cdot \frac{\partial}{\partial x} \left[u \cdot \frac{\partial C}{\partial t} \right] \right] - \frac{\tau}{2} \cdot \frac{\partial}{\partial x} \left[C \cdot \frac{\partial u}{\partial t} \right] \\
& - \frac{\tau^2}{6} \cdot \frac{\partial}{\partial x} \left[\frac{\partial}{\partial t} \left[C \cdot \frac{\partial u}{\partial t} \right] + \frac{\partial u}{\partial t} \cdot \frac{\partial C}{\partial t} + \frac{1}{2} \cdot u \cdot \frac{\partial}{\partial x} \left[C \cdot \frac{\partial u}{\partial t} \right] \right] = 0 \dots
\end{aligned} \quad (23)$$

Referring to this DA we develop the FDS with artificial dispersion, but only some terms are included in consideration with the last two being omitted. Like for the linear equation we study two FDSs (24) and (25) with artificial dispersion, analogous to (16) and (17) respectively:

$$C_i + (W_{i+1/2}^{(0.5)} - W_{i-1/2}^{(0.5)})/h - D \cdot C_{xx}^{(0.5)} + A + B + C = 0, \quad (24)$$

$$C_i + (W_{i+1/2}^{(0.5)} - W_{i-1/2}^{(0.5)})/h - D \cdot C_{xx}^{(0.5)} + A + B + C = 0, \quad (25)$$

where

$$A = -\frac{h^2}{6} \cdot \left[\alpha \cdot (u \cdot C^{(\sigma)})_{xxx} + (1 - \alpha) \cdot (u \cdot C_{xxx}^{(\sigma)}) \right],$$

$$B = \frac{h^2}{4} \cdot [u_x \cdot C_x^{(\sigma)}]_x,$$

$$C = \frac{\tau^2}{12 \cdot h} \cdot [u_{i+1/2} \cdot [u \cdot C_i]_x - u_{i-1/2} \cdot [u \cdot C_i]_x],$$

$$A^* = \frac{h^2}{6} \cdot C_{xxt}.$$

Schemes (24) and (25) were compared by Ermakov et al. (1990) using the test problem, when the velocity function was typical for ZE model:

$$u = \frac{u_0}{1 + \partial_c \cdot C}, \quad (\partial_c = \text{const}, u_0 = \text{const}). \quad (26)$$

The initial concentration profile C had the form of rectangular pulse. It was shown that in this case the FDS (25) had insufficient dissipation. Nonlinearity of equation (21) leads to situation when even the initially smooth concentration profile, becoming steeper

and steeper, reaches the so called gradient catastrophe in a finite time¹. From this moment the solution obtained by the FDS (25) demonstrates spurious oscillations behind the concentration drop, which are much similar to those shown in Fig. 3 for $t = 0.05$. The FDS (24) with $\kappa = 0$ does not yield in fact any oscillations, and the solution, like in linear case, contains only two small peaks in grid points just ahead and behind the shock. Therefore, for solving non-linear problems the FDS (24) is more preferable. Here and further referring to FDS (24) we shall assume this FDS with parameter $\kappa = 0$.

The FDS (24) was generalized by Ermakov et al. (1990) also for the case with two spatial dimensions.

3.3. The test problem: isotachophoresis (strong electrolytes). In this section we analyze the computational efficiency of FDS (24) compared to upwind FDS (27)

$$C_t + (u \cdot C^{(0.5)})_x = D \cdot C_{xx}^{(0.5)}, \quad (27)$$

like we do it in Sec. 3.1 for FDSs (16) and (12). However for this purpose we consider more complicated problem on ITP separation of two component sample using strong electrolytes' approximation. This approximation implies that the following simplifications in ITP mathematical model (Sec. 2) are adopted:

- (i) the electrolytes are fully dissociated;
- (ii) the contribution of hydrogen and hydroxyl ions to the total electric current in capillary (5) and the neutrality condition (6) is neglected;
- (iii) the counterion concentration is equal to $a_0 = \sum_i a_i$.

With these assumptions the problem is reduced to solving equations (4) for acids together with reduced relation for the current density (5).

¹ In this case the derivative of solution does not reach infinite values because the coefficient at the second derivative is not equal to zero, but the derivative is sufficiently great so that the characteristic drop of solution takes place on the space interval smaller than grid step h .

We assume that $n = 4$, i.e., the system consists of 5 components: the terminator, two sample species, the leader and the counterion. At the initial moment the concentration distribution is as follows: terminator electrolyte is composed of terminator-ion $a_1 = 1/3$ and counterion $a_0 = 1/3$; mixture includes two sample species $a_2 = 1/5$, $a_3 = 2/15$ and counterion $a_0 = 0.2$; the leader electrolyte is composed of leader-ion $a_4 = 0.2$ and counterion $a_0 = 0.2$. Initial concentration profiles along the capillary is schematically shown in Fig. 6. The ions' relative mobilities are equal to $\gamma_0 = 1.87$, $\gamma_1 = 1.00$, $\gamma_2 = 1.047$, $\gamma_3 = 1.97$, $\gamma_4 = 5.31$, while Schmidt numbers are $Sc_0 = 4.81 \cdot 10^2$, $Sc_1 = 9.01 \cdot 10^2$, $Sc_2 = 8.54 \cdot 10^2$, $Sc_3 = 4.52 \cdot 10^2$, $Sc_4 = 1.69 \cdot 10^2$ respectively. We assume that the capillary length equals 2cm, while its diameter is $d = 0.08$ cm. The system is maintained at the temperature $T = 291$ K, and the current density is constant and equal to $j = 497$ A/m². The sample volume is 2 microliter, that corresponds to 1/10 of the capillary length.

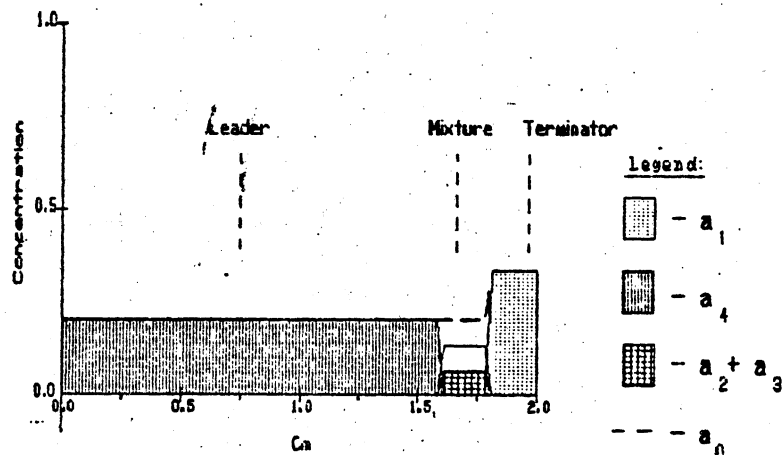


Fig. 6. Initial concentration profiles along capillary.

For solving the problem by means of FDSs (27) and (24) the uniform space and time difference grid was used. A system of linear equations with three or five diagonal matrix was solved for each time layer.

Fig. 7a, b display the concentration profiles at $t = 0.125$, ob-

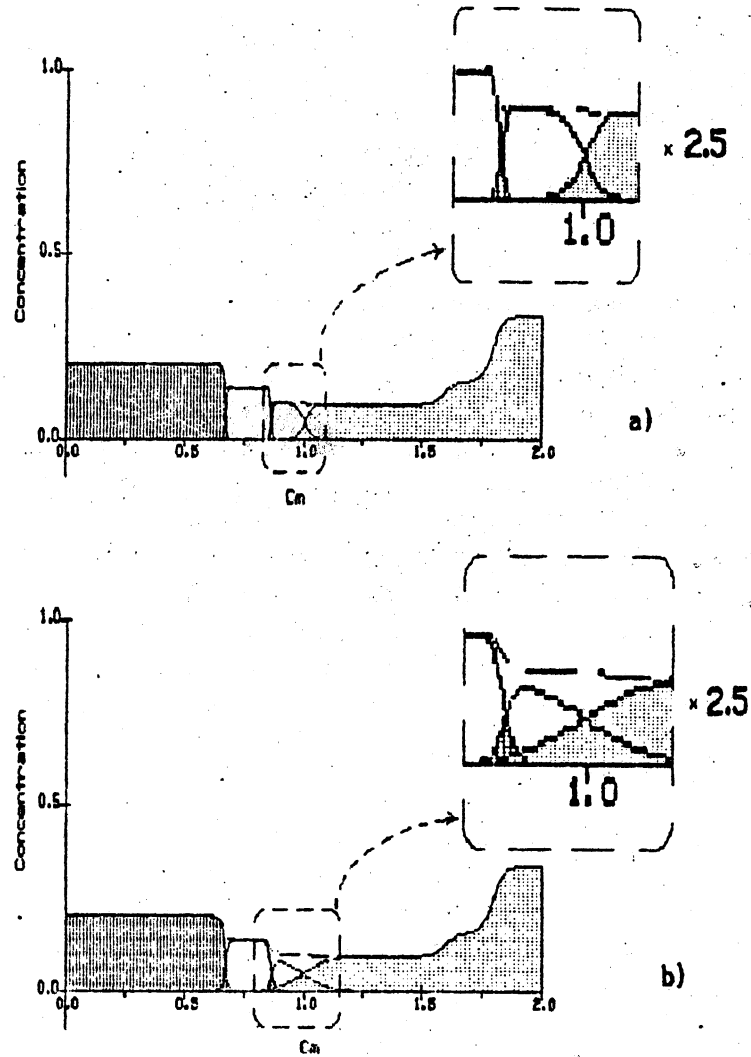


Fig. 7. Concentration profiles by $t = 0.125$: (a) using FDS (24); (b) using FDS (27).

tained using the FDSs (24) and (27) respectively. The designation of the substances is the same as in Fig. 6, the outlined fragments are zoomed. Though in both cases the computations were made

with $h = 5 \cdot 10^{-3}$ and $\tau = 5 \cdot 10^{-4}$, however the solutions are quite different. In Fig. 7a it can be observed that sample species are separated and there are only small regions where concentration profiles overlap. We may prove that this result is close to an exact solution by fulfilling computations on finer grids with the use of both schemes. The solutions will actually be the same as in Fig. 7a.

The computations with the scheme (27) give a different result: the slower component gets mixed up with the terminator, and the complete separation is not occurred. This is explained by the existence of considerable numerical diffusion. In order to obtain the solution which was as accurate as that shown in Fig. 7a, we used the space grid with $h = 5 \cdot 10^{-4}$. The computing time for FDS (24) when $h = 5 \cdot 10^{-3}$ starting from $t = 0.0$ up to $t = 0.1$ was equal to 86 sec., while the FDS (27) required 420 sec., i.e., about five times more. In the last case the time step was taken as large as possible to keep the computations stable. Moreover using a finer grid requires additional computer memory which is often limited. So we may conclude that the FDS (24) turns out to be more effective than (27) for solving the problems of given class, therefore we shall use it further in our simulation.

4. Simulation results. Now let's consider the results of simulation of the capillary ITP for the problem described in Sec. 3.3, but unlike that case we do not imply any simplifications. A mathematical model of the process is given in Sec. 2. All parameters, boundary and initial conditions are quite similar to those in Sec. 3.3 with the only exception: the concentrations of the sample species will be put equal to: $a_0 = 1$, $a_2 = 1/6$, $a_3 = 2/15$. Since the dissociation degrees α_i are not equal to unity now, we give the equilibrium constants $K_0 = 3.49 \cdot 10^{-8}$, $K_1 = 5.28 \cdot 10^{-8}$, $K_2 = 6.96 \cdot 10^{-8}$, $K_3 = 2.52 \cdot 10^{-7}$, $K_4 = 3.33 \cdot 10^7$. The hydrogen and hydroxyl mobilities are: $\gamma_5 = 24.36$ and $\gamma_6 = 13.76$; the corresponding dimensionless Schmidt numbers: $Sc_5 = 36.9$, $Sc_6 = 65.36$. Now the system of equations (4)–(6) is completely definite. Equations (4) are approximated using FDS (24), assuming that $W_i^{(0.5)} = z_i \cdot \alpha_i \cdot \gamma_i \cdot E \cdot a_i^{(0.5)}$ is mass flux

of i -th species, where E and α_i values are taken from the previous time step. This results in a system of linear equations which are solved for each time step using conventional Gauss routine. Equation (6) together with (3) and (9) may be written as nonlinear algebraic equation with respect to hydrogen concentration $[H^+]$:

$$f([H^+]) = \frac{z_0 \cdot a_0 \cdot [H^+]}{K_0 + [H^+]} + \sum_{i=1}^4 \frac{z_i \cdot a_i \cdot K_i}{K_i + [H^+]} + [H^+] - \left[\frac{K_w}{a^*} \right]^2 \cdot \frac{1}{[H^+]} = 0. \quad (28)$$

This equation may be solved by using the Newton iteration procedure. The function $f([H^+])$ is monotone, $f'([H^+]) > 0$ and $f''([H^+]) < 0$ for $[H^+] > 0$. (From the physical point of view we would be interested only in solutions which are greater than zero). Hence, if we take the start value $[H_0^+]$ so that $[H_0^+] < [H_r^+]$, where $[H_r^+]$ is the root of eq. (28), the iteration process would monotonically converge to $[H_r^+]$. We can always obtain such $[H_0^+]$ believing $[H_0^+] = 10^{-p}$ (where $p = 1, 2, \dots$ - are natural numbers) and increasing p until $f([H^+])$ becomes less than zero.

The solution process was fulfilled in the following sequence: by taking the known distribution a_i from the previous time step we calculated the distribution $[H^+]$; then the electric field intensity E was calculated using (5), and finally equations (4) were solved for each component. This sequence was repeated in the next time step. The calculations were fulfilled using grid with $h = 2 \cdot 10^{-3}$ and $\tau = 10^{-4}$.

Capillary ITP simulation results are presented in Fig. 8-10. Evolution of concentration profiles for three time moments is shown in Fig. 8a-c (the initial distribution is similar to that in Fig. 6. except for concentration values for sample species). Fig. 8a, b correspond to separation process, while Fig. 8c displays the final stage, when the sample species separate into so-called "clear" zones. The boundaries between the individual components are sufficiently sharp, their diffusion distortion is small. The analysis of the results obtained and their comparison with the diffusionless model (Zhukov, 1984) demonstrates good agreement. For example, comparing the electrolyte concentrations at the final stage, the length

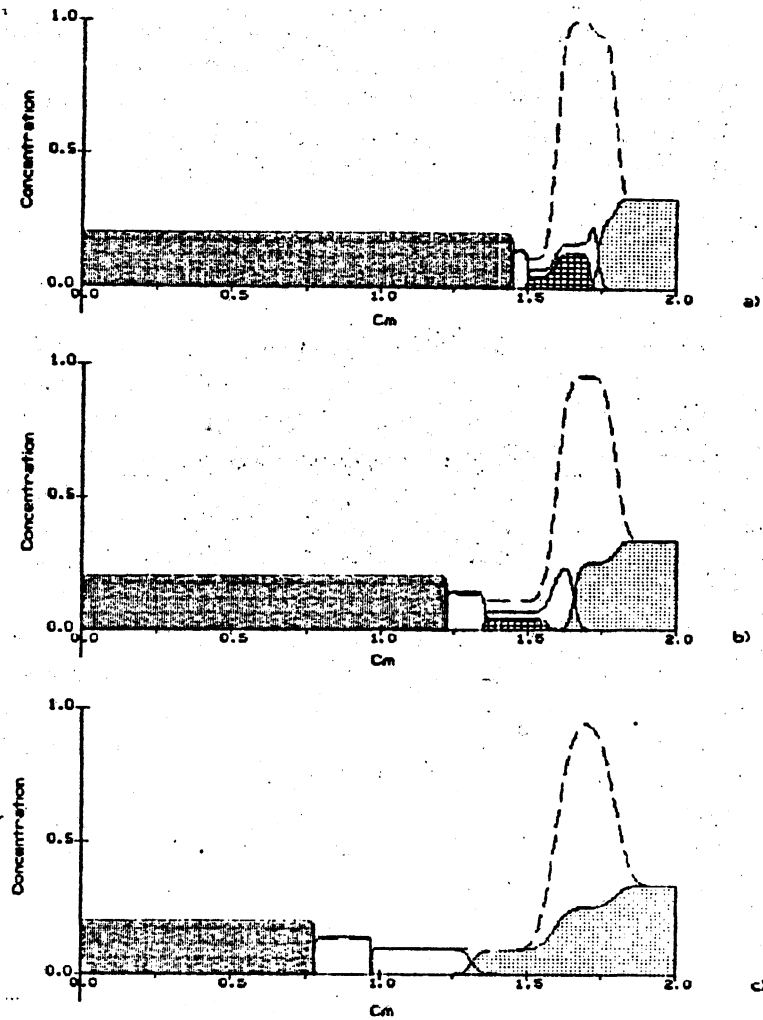


Fig. 8. Evolution of concentration profiles during ITP separation.

of individual zones as well as the time of complete separation, we obtained that in all cases deviations in data do not exceed 1 percent. Both models give very similar results concerning the dynam-

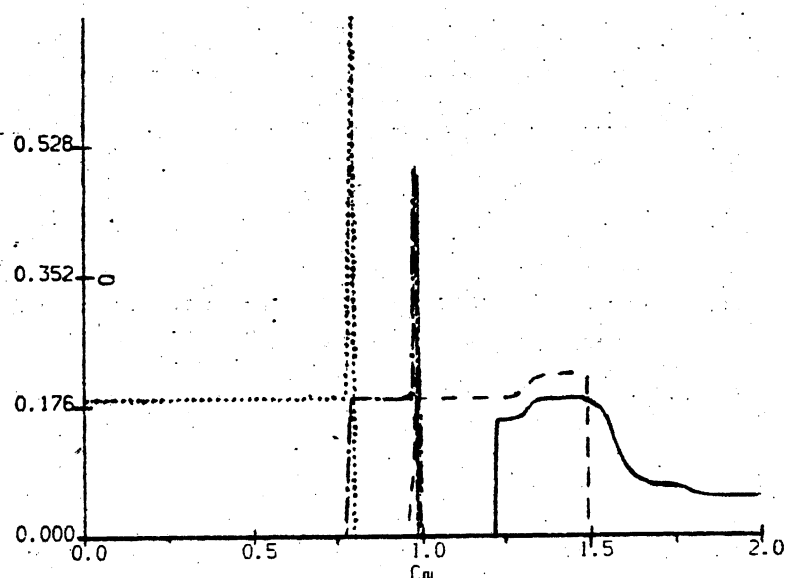


Fig. 9. Equivalent velocity $Q = u_i \cdot \tau / h$ profiles along capillary.
 Components: ——— $i = 1$, - - - - - $i = 2$, - · - · - $i = 3$, · · · · · $i = 4$.

ics of separation. It is proved by the identity of time moments at which the rear front of each sample species crosses the point of so-called steady shock ($x = 1.6\text{cm}$, Fig. 8c). The existence of steady concentration shocks was predicted by Zhukov (1984) in his diffusionless model, and, as we've convinced, the diffusion didn't change the situation considerably. All this facts on one hand demonstrate the small influence of diffusion on the transport of sample, while, on the other hand they prove the high accuracy of the developed algorithm.

Fig. 9 shows the profiles of dimensionless net velocity for every component multiplied by time/space grid steps ratio, i.e., $q = u_i \cdot \tau / h^1$. This product is the Courant number. The stability of an explicit numerical algorithms for hyperbolic equation is usually

¹ We assume $u_i = 0$ whenever the concentration a_i is less than 10^{-3} .

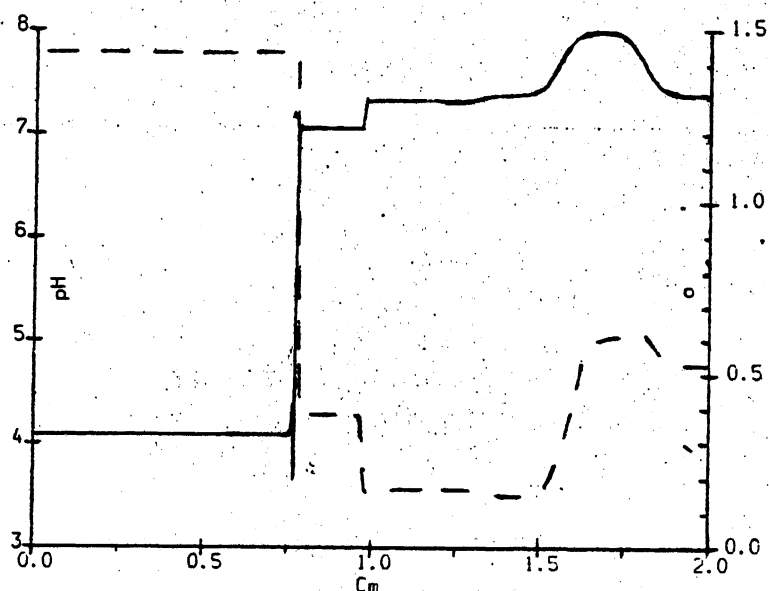


Fig. 10. Conductivity σ ----- and pH value ——— profiles by $t = 0.11$; $pH = -\log_{10}([H^+])$.

estimated by a limiting value of the Courant number. We took $\tau/h = 0.05$, and the time step may seem to be very small. However it is not so, since the dimensionless velocity u_i is much more than unity and $q \approx 1$. Numerical experiments with different τ/h ratio showed that computations remained stable until $q \leq 2$. The maximum u_i values were observed near the boundaries between solution components, where they underwent the shocks. Simultaneously the velocities were constant in the regions with steady concentration and their values were equal to Kohlrausch migration velocity at the final stage of the process. The identical migration velocity for the species with different mobilities is achieved due to variation of electric field intensity along capillary. In the regions with slower components the field intensity is greater, while the conductivity is lower. The conductivity profile together with hydrogen ion $[H^+]$ distribution along capillary by $t = 0.11$ is plotted in Fig. 10. Though the relative hydrogen concentration is subjected to con-

siderable variations along the capillary, its absolute value remains small, compared to those for other components. Hence, the hydrogen ions make insignificant contribution to the total current (5) and electric neutrality relation (6). So a behavior of a system will be much similar the case of strong electrolyte (Sec. 3.3.). The situation, however, may change if the initial distribution of electrolyte is different, for example, if concentration of the counterion is lower than that of the leader.

5. Conclusions. In this paper the results of computer simulation on capillary ITP separation are presented. The efficient numerical algorithm based on the FDS with artificial dispersion has been developed. It enables to solve the convection-diffusion equations with small coefficient at the second derivative, using difference grids with relatively small number of nodes. In this case for a prescribed accuracy the computation time may be reduced, what has been confirmed by test computations. Based on given approach 1-D numerical code was developed for numerical simulation of capillary ITP. One of the main results of this study concerns the estimation of diffusion effect on the sample boundary spreading. This code may be also applied to investigation of another capillary electrophoresis technique—zone electrophoresis.

REFERENCES

- Babskii, V.G., M.Yu.Zhukov and V.I.Yudovich (1989). *Mathematical Theory of Electrophoresis*. Consultants Bureau, New York. 241pp.
- Bier, M., O.A.Paluszinski, A.Mosher and D.A.Saville (1983). Electrophoresis: Mathematical modeling and computer simulation. *Science*, **219**(4590), 1281–1287.
- Deyl, Z. (Ed.) (1979). *Electrophoresis: A Survey of Techniques and Applications*. Elsevier, Amsterdam. 350pp.
- Ermakov, S.V., O.S.Mazhorova and Yu.P.Popov (1990). *Construction of FD Schemes for Parabolic Equation with Small Parameter at the Higher Derivative*. Keldysh Inst.Appl.Math. USSR Acad.Sci. Preprint, # 89. 28pp. (in Russian).
- Filder, Z., V.Filder and J.Vacik (1985). Dynamics of isotachophoretic separation. II. Impurities in the electrolytes and sample injection. *J.Chromato-*

- graphy*, **320**, 175-183.
- Mazhorova, O.S., Yu.P.Popov and V.I.Pohilko (1986). *FD Scheme with Artificial Dispersion for Parabolic Equation*. Keldysh Inst.Appl.Math. USSR Acad.Sci. Preprint, # 142. 26pp. (in Russian).
- Mosher, R.A., D.Dewey, W.Thormann, D.A.Saville and M.Bier (1989). Computer simulation and experimental validation of the electrophoretic behavior of proteins. *Analytical Chemistry*, **61**(4), 362-366.
- R.A.Mosher, W.Thormann and M.Bier (1985). Computer aided analysis of electric field gradients within electrophoretic boundaries between weak electrolytes. *J. Chromatography*, **320**, 23-32.
- Muhin, S.I., S.B.Popov and Yu.P.Popov (1981). *Dispersion and Dissipative Properties of FD Schemes for Nonlinear Transport Equation*. Keldysh Inst.Appl. Math. USSR Acad.Sci. Preprint, # 150. 28pp. (in Russian).
- Roberts, G.O., and R.S.Snyder (1989). Dispersion effects in capillary zone electrophoresis. *Journal of Chromatography*, **480**, 35-67.
- Saville, D.A., and O.A.Paluszinski (1986). Theory of electrophoretic separation. Part I: Formulation of a mathematical model. *AIChE Journal*, **32**(2), 207-214.
- Shokin, Y.I., and N.N.Yanenko (1985). *Method of Differential Approximation*. Nauka, Novosibirsk. 364pp. (in Russian).
- Zhukov, M.Yu. (1984). Nonsteady isotachophoresis model. *Zhurnal Vychislitel'noy Matematiki i Matematicheskoi Fiziki*, **24**(4), 549-565 (in Russian).

Received September 1991

S. Ermakov received the Degree of Candidate of Physico-Mathematical Sciences from Moscow Physico-Technical Institute, USSR, in 1988. He is a researcher at Keldysh Institute of Applied Mathematics the USSR Academy of Sciences in Moscow. His scientific interests concern the finite-difference algorithms for simulation of heat and mass transfer processes.

O. Mazhorova received the Degree of Candidate on Physics and Mathematics from the Moscow Physico-Technical Institute USSR, in 1980. She is a senior researcher at Keldysh Institute of Applied Mathematics the USSR Academy of Sciences in Moscow. Her scientific interests include the numerical methods for simulation in hydrodynamics, heat and mass transfer applied to technological processes.

Yu. Popov received the Doctor Degree on Physics and Mathematics from the Moscow University, USSR in 1980. He is a professor in Moscow University. He is a deputy director at Keldysh Institute of Applied Mathematics the USSR Academy of Sciences. His main scientific interests are dealt with theory of finite-difference schemes and numerical methods, simulation and its scientific application.